Control of across-wind vortex shedding induced vibrations in tall buildings using the tuned mass-damper-inerter (TMDI)

Francesco Petrini[1], Agathoklis Giaralis[2]*

[1] *Sapienza University of Rome, Rome, ITALY*

[2] *Department of Civil Engineering, City University London, London, UK*

ABSTRACT

In this paper, the effectiveness of the tuned mass-damper-inerter (TMDI) vis-à-vis the classical tuned mass-damper (TMD) is assessed to suppress vortex shedding induced vibrations to tall building structures in the across-wind direction. The TMDI, previously proposed in the literature to mitigate earthquake-induced vibrations in multi-storey buildings, benefits from the mass amplification effect of the inerter (i.e., a two-terminal device developing a resisting force proportional to the relative acceleration of its terminals by the inertance constant) to achieve improved vibration suppression performance from the classical TMD for the same attached mass. Herein, a linear reduced-order structural system is developed, defined by a diagonal mass matrix and full damping and stiffness matrices, which captures faithfully the dynamic properties of a detailed finite element model corresponding to a benchmark 74-storey building with square floor plan. A TMDI is added to the structural system by elementary operations to the mass, damping, and stiffness matrices under the assumption of an ideal linear inerter. The wind action is represented by an analytical spectral density matrix modelling correlated across-wind induced forces accounting for vortex shedding and the structural analysis step is undertaken in the frequency domain for efficiency. A comprehensive parametric analysis is undertaken demonstrating that the TMDI achieves better performance in terms of peak top floor acceleration reduction with increasing inertance than a classical TMD with the same attached mass. This is also true for relatively small attached masses of practical interest to tall buildings (less than 0.5% the total buildings mass) for the case of peak top floor displacements. Further, it is shown that the TMDI reduces significantly the peak attached mass displacement, while the peak developing forces at the inerter are not excessive and can be locally accommodated by the building.

Keywords: *Tall buildings, vortex shedding, tuned mass damper, inerter, wind*

1 INTRODUCTION

Slender high-rise buildings with rectangular floor plan may experience excessive oscillations in the across-wind direction (i.e., within the normal plane to the wind direction) due to vortex shedding effects generated around their edges (see e.g. [1]). In fact, in many cases, vortex shedding induces higher peak floor accelerations in slender/tall buildings in the across-wind direction than those exhibited in the along-wind direction ([2], [3]). In such cases, ensuring that the across-wind floor accelerations remain below a certain threshold becomes the critical requirement in the design

[1] Post-Doctoral Fellow, francesco.petrini@uniroma1.it

[2] Senior Lecturer, agathoklis@city.ac.uk

* Corresponding author

of slender buildings at a serviceability limit state. This is because floor accelerations is closely associated with occupants' comfort ([4]).

In this context, over the past three decades, tuned mass dampers (TMDs), among other devices and configurations for supplemental damping, have been widely used in practice for vibration mitigation in wind-excited tall buildings to meet occupants' comfort performance criteria prescribed by building codes and guidelines ([5], [6]). In its simplest form, the linear passive TMD comprises a mass attached towards the top of the building whose oscillatory motion is to be controlled (primary structure) via optimally designed/"tuned" linear stiffeners, or hangers in case of pendulum-like TMD implementations, in conjunction with linear energy dissipation devices (dampers). The effectiveness of the TMD relies on "tuning" its stiffness and damping properties for a given primary structure and attached mass, such that significant kinetic energy is transferred from the vibrating primary structure to the TMD mass and eventually dissipated through the damping devices. Focusing on the suppression of lateral wind-induced vibrations, the TMD is tuned to the first natural frequency of the primary structure aiming to control the fundamental (translational) lateral mode shape (e.g. [7], [8]).

It is well-understood that the performance of TMDs depends heavily on its inertia property: the larger the attached TMD mass that can be accommodated by the primary structure subject to structural design and architectural constraints (e.g. in typical tall building applications the attached mass usually ranges in between 0.3%-1.5% of the total building mass), the more effective and robust to uncertainties the TMD becomes for passive vibration control (e.g. [9]). In this regard, recently, a generalization of the classical passive TMD incorporating an inerter device has been proposed in [10] and [11] for vibration suppression of base-excited multi-storey buildings termed the tuned mass-damper-inerter (TMDI). The inerter is a two-terminal device developing a resisting force proportional to the relative acceleration of its terminals ([12]). The underlying constant of proportionality (inertance) can be orders of magnitude larger than the physical mass of the inerter ([13), which, therefore, can be viewed as a mass amplification device. In this respect, it has been shown that the TMDI is more effective to mitigate seismically induced oscillations compared to the classical TMD for the same attached mass by relying on the mass amplification effect of the inerter device ([11]).

In this paper, the potential of the TMDI to suppress vortex shedding induced vibrations in tall buildings vis-à-vis the classical TMD is assessed. This is accomplished by undertaking a parametric study involving a typical (benchmark) 74-storey building (primary structure) equipped with TMDIs of various attached mass and inertance values and exposed to across-wind excitation which includes vortex shedding effects. The structural analysis step is undertaken in the frequency domain and is expedited by modelling the primary structure as a reduced-order lumped-mass linear dynamical system extracted from a detailed finite element model (FE). Further, this modelling approach allows for the incorporation of the TMDI to the primary structure in a straightforward manner.

The remainder of the paper is organised as follows. Section 2 offers a brief review of the TMDI for multi-storey buildings modelled as lumped-mass linear damped dynamical systems. Section 3 describes the adopted benchmark primary structure and its dynamical modelling along with the considered wind input action represented by a power spectral density function. Section 4 furnishes and discusses novel numerical data in terms of peak top floor displacement and acceleration, attached mass displacement (stroke), and developing inerter force as functions of inertance and for different values of fixed TMDI mass. Finally, conclusions are summarised in section 5.

2 THE TUNED MASS-DAMPER-INERTER (TMDI) FOR MULTI-STOREY BUILDINGS

Conceptually introduced by [12], the ideal inerter is a linear two terminal device of negligible mass/weight developing an internal (resisting) force F proportional to the relative acceleration of its terminals which are free to move independently. Its resisting force is expressed as

$$F = b(\ddot{u}_1 - \ddot{u}_2), \tag{1}$$

where u_1 and u_2 are the displacement coordinates of the inerter terminals as shown in the inlet of Fig. 1 and, hereafter, a dot over a symbol signifies differentiation with respect to time. In the above equation, the constant of proportionality b is the so-called inertance and has mass units; it fully characterizes the behaviour of the ideal (linear) inerter. Importantly, the physical mass of actual inerter devices can be two or more orders of magnitude lower than b. This has been experimentally validated by testing several different prototyped inerter devices proposed in the literature ([13], [14], [15]). In this regard, the ideal inerter can be construed as an inertial amplification device, since by "grounding" any one of its terminals, the device acts as a "weightless" mass b ([12]).

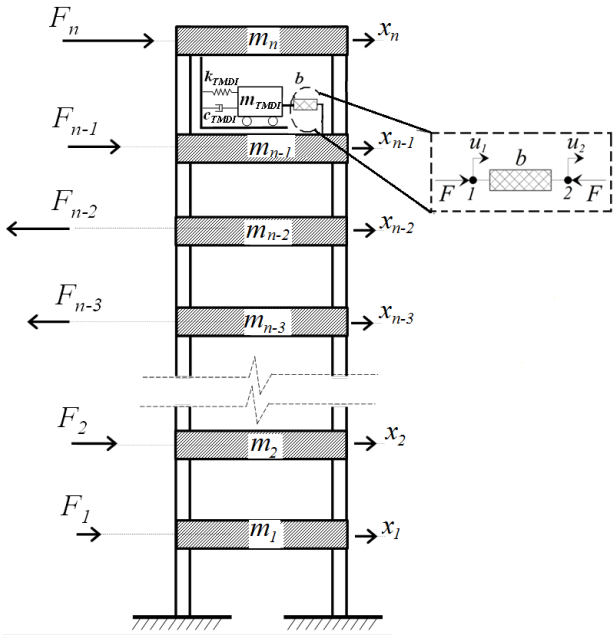

Figure 1 - Lumped-mass model of a tuned mass-damper-inerter (TMDI) equipped n-storey building subject to arbitrary (instantaneous) lateral wind forces and schematic representation of an inerter device subject to an external force F.

$$\mathbf{M} = \begin{bmatrix} m_1 & 0 & \cdots & \cdots & \cdots & 0 \\ 0 & m_2 & \cdots & \cdots & \cdots & \vdots \\ \vdots & \vdots & \ddots & 0 & 0 & 0 \\ \vdots & \vdots & 0 & m_{n-1}+b & 0 & -b \\ \vdots & \vdots & 0 & 0 & m_n & 0 \\ 0 & \cdots & 0 & -b & 0 & m_{TMDI}+b \end{bmatrix}, \mathbf{C} = \begin{bmatrix} c_{1,1} & c_{1,2} & \cdots & \cdots & c_{1,n} & 0 \\ & c_{2,2} & \cdots & \cdots & \vdots & \vdots \\ & & \ddots & c_{n-2,n-1} & c_{n-2,n} & 0 \\ & & & c_{n-1,n-1} & c_{n-1,n} & 0 \\ & SYM & & & c_{n,n}+c_{TMDI} & -c_{TMDI} \\ & & & & & c_{TMDI} \end{bmatrix}, \tag{2}$$

$$\text{and} \quad \mathbf{K} = \begin{bmatrix} k_{1,1} & k_{1,2} & \cdots & \cdots & k_{1,n} & 0 \\ & k_{2,2} & \cdots & \cdots & \vdots & \vdots \\ & & \ddots & k_{n-2,n-1} & k_{n-2,n} & 0 \\ & & & k_{n-1,n-1} & k_{n-1,n} & 0 \\ & SYM & & & k_{n,n}+k_{TMDI} & -k_{TMDI} \\ & & & & & k_{TMDI} \end{bmatrix}$$

Shown in Fig. 1 for a planar n-storey building primary structure modelled as a lumped-mass n degree-of-freedom (DOF) system, the tuned mass-damper-inerter (TMDI) proposed in [10] and [11] () exploits the aforementioned mass amplification property of the inerter device to enhance the vibration suppression capabilities of the classical TMD. Specifically, in the herein considered topology, the TMDI comprises a mass m_{TMDI} attached to the top floor of the primary structure via a linear spring of stiffness k_{TMDI} and a linear dashpot of damping coefficient c_{TMDI}, and linked to the penultimate floor by an ideal linear inerter inertance b. The mass **M**, the damping **C**, and the stiffness **K** matrices characterizing the dynamic behaviour of the TMDI equipped system in Fig. 1 are given in Eq. (2) shown in the bottom of the previous page, where m_i is the mass of i-th floor (i=1,2,…,n), and $c_{i,j}$ and $k_{i,j}$ are the (i,j) elements of the primary structure damping and stiffness matrices, respectively.

Note that for $b=0$, the matrices in (2) correspond to a building structure having a classical TMD attached to its top floor. The latter TMD topology is widely considered to control the first mode of vibration of multi-storey buildings which, for regular in elevation structures, dominates their dynamic response to lateral dynamic loads. It is further important to note that the inclusion of the inerter device alters only the mass matrix which is no longer diagonal. Indeed, the inerter not only does it contribute to the mass corresponding to the DOF of the attached mass and of the penultimate floor, but also introduces "gyroscopic" inertia cross-terms that couples the aforementioned DOFs. The latter alters effectively the dynamics of the primary structure in a manner that dampens higher modes of vibration and not only the fundamental one ([16]).

The fact that the effective inertia corresponding to the DOF of the attached mass is equal to (m_{TMDI}+b) motivates the definition of the following dimensionless frequency ratio υ_{TMDI} and damping ratio ξ_{TMDI}

$$\upsilon_{TMDI} = \frac{\sqrt{\frac{k_{TMDI}}{(m_{TMDI}+b)}}}{\omega_1} \quad , \; \xi_{TMDI} = \frac{c_{TMDI}}{2\sqrt{(m_{TMDI}+b)k_{TMDI}}}, \tag{3}$$

to characterize the dynamics of the TMDI given an attached mass m_{TDMI} and inertance b. In the last equation ω_1 is the first (fundamental) natural frequency of the primary (uncontrolled) structure.

3 PRIMARY STRUCTURE AND WIND EXCITATION MODELLING

3.1 Benchmark 74-storey building description and detailed FE modelling

In assessing the potential of the TMDI in Fig. 1 to suppress vortex shedding induced oscillations in tall buildings in the across-wind direction, a high-rise building utilized before for the development of a performance-based wind engineering framework ([17], [18]) is taken as a benchmark case-study. The adopted structure is a 74-storey steel frame building of 305m total height with a 50m-by-50m square floor plan. Its lateral load resisting system comprises two spatial steel frames, one inner (core) and one outer (perimetric), connected together by three outriggers located at 100m, 200m, and 300m in elevation. The core frame includes 16 columns, while the perimetric frame has 28 columns. All columns have hollow square sections, with outer dimensions and thickness varying with the height and ranging in between 1.20m to 0.50m, and 0.06m to 0.025m, respectively. Beams are of various standard double-T steel section profiles and all beam-to-column joints are taken as rigid. The bracing system of the outriggers is composed by double-T or hollow-square struts and spans 2 or 3 stories.

A detailed linear FE model of the lateral load resisting structural system is developed in SAP2000 commercial FE package. An extruded three-dimensional snapshot of the total model is shown in Fig. 3(a), while Fig. 3(b) shows the FE model of a 2-story outrigger. The FE model consists of 7592 linear Euler-Bernoulli beam elements with pinned or hinged connections as

appropriate. Horizontal perfectly rigid diaphragm constraints are imposed at the height of each floor to account for the effects of the slabs in the model. The mass and gravitational loads carried by each slab are uniformly distributed and lumped at the nodes of the FE model.

Standard linear modal analysis is undertaken using the above FE model to determine the mode shapes and natural frequencies of the benchmark structure. In Fig. 2(c) the first three dominantly translational mode shapes along a principal axis of the (double symmetric in plan) structure are plotted. The corresponding natural frequencies or periods, and the modal participating mass ratios (MPMRs) are reported in Table 1. In the following sub-section the obtained mode shapes from the detailed FE model are used, together with an assumed diagonal mass matrix, to derive a reduced-order dynamical model which captures faithfully the dynamic response of the adopted benchmark structure within a vertical plane of symmetry due to lateral wind induced time-varying forces.

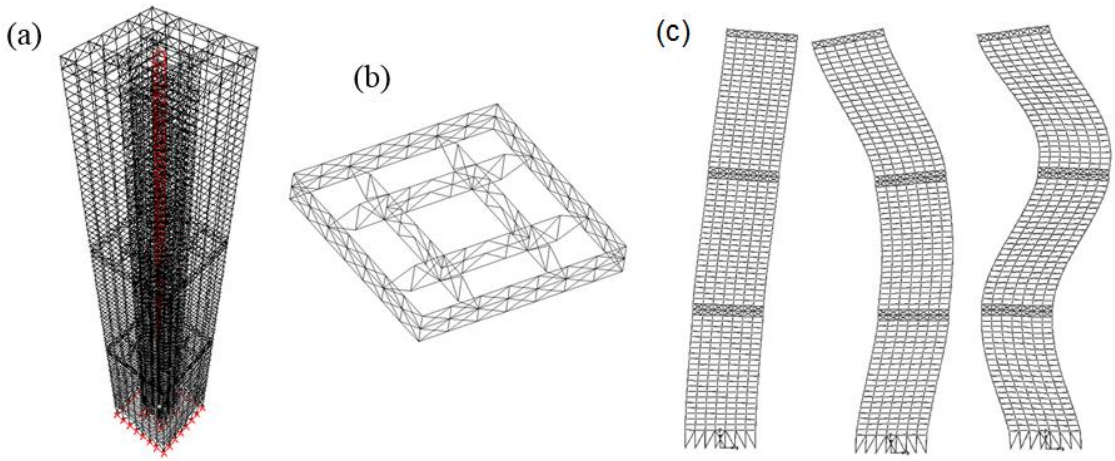

Figure 2- (a) FE model of the benchmark 74-story building, (b) FE model of a two-story outrigger, (c) Side planar view of the first three lateral translational mode shapes

Table 1: Natural frequencies, natural periods and modal participating factors of the first three lateral translational mode shapes of the FE model in Fig. 2

Mode	***n* [Hz]**	***ω* [rad/s]**	***T* [sec]**	**MPMR**
1	0.18515	1.1634	5.40	0.6233
2	0.56335	3.5396	1.77	0.1900
3	1.0518	6.6088	0.95	0.0745

3.2 Reduced primary structure model

Based on the detailed FE model presented in the previous sub-section, a simplified planar dynamical model with 74 dynamic degrees of freedom (DOFs) is herein defined in terms of a mass $\mathbf{M}_{(0)}$, damping $\mathbf{C}_{(0)}$, and stiffness $\mathbf{K}_{(0)}$ matrices to be treated as the primary structure. In particular, a reduced diagonal 74-by-74 mass matrix $\mathbf{M}_{(0)}$ is firstly defined under the assumption of lumped masses at each floor level equal to 1250ton. The mass of the structural elements are accounted for in this value including the mass of columns equally divided between consecutive floors. Further, a full 74-by-74 stiffness matrix $\mathbf{K}_{(0)}$ is obtained such that it satisfies the following system of equations of standard modal analysis

$$\left[\mathbf{K}_{(0)} - \omega^2_{(\mathrm{FEM})_j}\mathbf{M}_{(0)}\right]\boldsymbol{\varphi}_{(\mathrm{FEM})_j} = 0 \quad ; \quad j = 1,2,...,74. \tag{4}$$

In the last equation $\boldsymbol{\varphi}_{(FEM)j}$ and $\omega_{(FEM)j}$ are the j-th translational mode shape in the across-wind direction (principal axis of building) and the corresponding natural frequency, respectively, obtained by the detailed FE model described in the previous sub-section. This was achieved by means of standard modal analysis upon constraining all rotational and translational DOFs along one of the two horizontal principal axes of the building at master nodes assigned to each floor. The choice of accounting for all the 74 mode shapes purely translational along one principal axis of the building has been made to capture the local dynamics of the structure near the outriggers, to maintain the DOFs of the top and the penultimate floors where the TMDI is connected to, and to ensure a fine discretization of the wind loading along the height of the building.

Lastly, a full $\mathbf{C}_{(0)}$ damping matrix is obtained from the expression ([19])

$$\mathbf{C}_{(0)} = \left(\boldsymbol{\Phi}^T\right)^{-1} \mathbf{C}_{\text{mod}} \left(\boldsymbol{\Phi}\right)^{-1}, \tag{5}$$

where $\boldsymbol{\Phi}$ is the 74-by-74 mode shape matrix collecting the $\boldsymbol{\varphi}_{(FEM)j}$ mode shapes and $\mathbf{C}_{\text{mod}}$ is the diagonal matrix containing the modal damping coefficients

$$c_j = 2\omega_j \xi_j \left(\boldsymbol{\varphi}_j{}^T \mathbf{M}_{(0)} \boldsymbol{\varphi}_j\right). \tag{6}$$

In the last equation, ξ_j is the j-th modal damping ratio, assumed as follow: 2% for j= 1 to 3, 4% for j= 4 to 6, 6% for j= 7 to 10, 9% for j= 11 to 20, 12% for j= 21 to 40, 15% for j= 41 to 60, 18% for the rest of the higher modes (j=61 to 74).

Note that the consideration of the above $\mathbf{M}_{(0)}$, $\mathbf{C}_{(0)}$, and $\mathbf{K}_{(0)}$ model is necessary as it allows to incorporate the TMDI and especially the inerter which, to the best of the authors' knowledge, is not currently contained in the element library of any structural analysis FE software, in a straightforward manner as suggested by Eq. (2). That is, by adding a DOF (i.e., a row and a column) together with the additional stiffness k_{TMDI}, damping c_{TMDI}, and inertial m_{TMDI} and b contributions of the TMDI to the $\mathbf{M}_{(0)}$, $\mathbf{C}_{(0)}$, and $\mathbf{K}_{(0)}$. The resulting model of the primary structure plus TMDI represented by the $\mathbf{M}$, $\mathbf{C}$, and $\mathbf{K}$ matrices in (2) can be readily used in conducting frequency domain structural analysis in any high-level computer language (e.g., MATLAB) in a computationally efficient manner as described in the following sub-section.

3.3 Wind model and Frequency domain approach for building response evaluation

For the purposes of this work, the wind action is considered only in the across-wind direction as this is the critical one for the occupants' comfort criterion for the particular benchmark primary structure ([18]). This is modelled as a zero-mean Gaussian ergodic stochastic process represented in the frequency domain by the 74-by-74 power spectral density matrix $\mathbf{S}_{\mathbf{FF}(0)}$ which collects all wind force components acting to each of the 74 floors (i.e., as a function of the height of the building) accounting for both wind turbulence and vortex shedding effects.

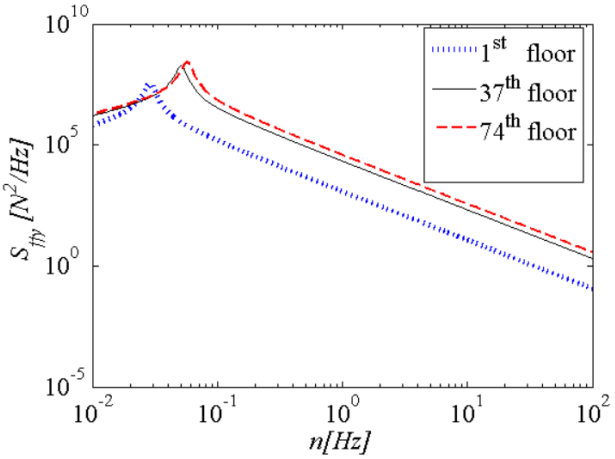

Figure 3- Considered across-wind force spectra at three different floors.

Specifically, the elements of the $\mathbf{S_{FF}}_{(0)}$ matrix are evaluated using the parametric formulae derived in [1] based on experimental wind tunnel data involving rectangular cylinders of various side ratios. The considered benchmark building has a square floor plan and, therefore, the 1:1 side ratio case is taken. Examples of across-wind force power spectral density functions evaluated at three different heights are shown in Fig. 3 assuming mean wind velocity at the top floor equal to 35m/s.

The PSD matrices of the displacement and the acceleration response of the TMDI equipped primary structure defined in the previous sub-section excited by the above wind force PSD matrix are obtained using the frequency domain input-output relationships of random vibrations [20]

$$\mathbf{S_{xx}}(\omega) = \mathbf{B}(\omega)^{*}\,\mathbf{S_{FF}}(\omega)\mathbf{B}(\omega) \tag{7}$$

and

$$\mathbf{S_{\ddot{x}\ddot{x}}}(\omega) = \omega^4 \mathbf{S_{xx}}(\omega), \tag{8}$$

respectively. In Eq. (7), $\mathbf{S_{FF}}$ is the PSD wind force matrix $\mathbf{S_{FF}}_{(0)}$ augmented by a zero row and a zero column corresponding to the DOF of the TMDI which is not subjected to any wind load, the (*) superscript denotes complex matrix conjugation, and the transfer matrix $\mathbf{B}$ is given as

$$\mathbf{B}(\omega) = \left[\mathbf{K} - \omega^2\mathbf{M} + i\omega\mathbf{C}\right]^{-1}. \tag{9}$$

In the last equation, $i = \sqrt{-1}$ and the (-1) superscript denotes matrix inversion.

Further, the response displacement and acceleration variances of the *k*-th floor for the TMDI equipped primary structure are obtained as

$$\sigma_{x_k}^2 = \int_0^{\omega_{\max}} S_{x_k x_k}(\omega)\, d\omega \tag{10}$$

and

$$\sigma_{\ddot{x}_k}^2 = \int_0^{\omega_{\max}} S_{\ddot{x}_k \ddot{x}_k}(\omega)\, d\omega, \tag{11}$$

respectively. That is, by integrating the response auto-spectra populating the main diagonal (*k*,*k*) elements of the response PSDs in Eqs. (7) and (8), along the frequency axis up a maximum (cut-off) frequency ω_{max} above which the energy of the underlying processes is negligible. Moreover, the variance of the relative acceleration response between two different floors *k* and *n* is obtained by

$$\sigma_{\ddot{x}_{kn}}^2 = \sigma_{\ddot{x}_k}^2 + \sigma_{\ddot{x}_n}^2 - 2\int_0^{\omega_{\max}} S_{\ddot{x}_k \ddot{x}_n}(\omega)\, d\omega, \tag{12}$$

where the integrand is the acceleration response cross-spectrum corresponding to the *k* and *n* DOFs.

Finally, peak *k*-th floor displacements and accelerations and peak relative acceleration between floors, or more generally between DOFs, *k* and *n* are estimated by the expressions

$$\max\{x_k\} = g\sqrt{\sigma_{x_k}^2}, \quad \max\{\ddot{x}_k\} = g\sqrt{\sigma_{\ddot{x}_k}^2}, \quad \text{and} \quad \max\{\ddot{x}_{kn}\} = g\sqrt{\sigma_{\ddot{x}_{kn}}^2}, \tag{13}$$

respectively. In the above expressions, *g* is the peak factor estimated by the following widely used in wind engineering applications empirical formulae due to Davenport [21]

$$g = \sqrt{2ln(\eta T_{wind})} + \frac{0.577}{\sqrt{2ln(\eta T_{wind})}}, \tag{14}$$

where $\eta=2\pi/\omega$ is the effective structural response frequency in Hz (e.g., can be assumed equal to the fundamental natural frequency of the primary structure), and T_{wind} is the assumed time duration of exposure to the wind action during which the maximum response quantities in (13) are evaluated. The latter consideration implies that the underlying stochastic input/output processes are quasi-stationary (i.e., stationary/ergodic time-limited processes).

In the following section, the peak response quantities in (13) are used to assess the effectiveness of the TMDI to suppress wind induced vibrations in tall buildings.

4 PARAMETRIC ANALYSIS AND DISCUSSION

A parametric investigation is herein conducted to explore the potential of the TMDI reviewed in section 2 to mitigate vibrations in the across-wind direction of tall buildings due to wind induced forces modelled by the spectra in Fig. 3. To this aim, the dynamical model defined in terms of the $\mathbf{M}_{(0)}$, $\mathbf{C}_{(0)}$, and $\mathbf{K}_{(0)}$ matrices in section 3.2 is adopted as the given primary structure which captures the in-plane lateral oscillatory response of the 74-storey building reviewed in section 3.1 represented via the therein detailed linear FE model. Furthermore, the wind induced lateral forces in the across-wind direction of the building are modelled by the PSD of Fig. 3 which assumes a mean wind velocity at the top floor equal to 35m/s. The structural analysis step is undertaken in the frequency domain as detailed in section 3.3 to obtain the peak structural response quantities in (13) assuming one hour of exposure to the wind action, that is, T_{wind} = 3600s in (14). Further, the effective frequency value in (14) is taken equal to the fundamental natural frequency of the adopted primary structure, that is, η= 0.185Hz (see also Table 1), which results in a peak factor value g= 3.97.

Six different values of the attached TMDI mass equal to 0.3%, 0.5%, 0.8%, 1%, 1.2%, and 1.5% of the total primary structure mass are considered in the parametric study. Further, the inertance b value is let to vary in the range of 0% to 100% of the total building mass, with the special case of b=0 being the same as the classical TMD. In all cases considered, the values of the TMDI frequency and damping ratios in (3) are obtained from the expressions

$$\upsilon_{TMDI}=\frac{\sqrt{1+0.5(\beta+\mu)}}{1+\beta+\mu} \quad \text{and} \quad \xi_{TMDI}=\sqrt{\frac{(\beta+\mu)\left[1+0.75(\beta+\mu)\right]}{4(1+\beta+\mu)\left[1+0.5(\beta+\mu)\right]}}, \tag{15}$$

respectively, where μ= m_{TMDI}/M and $\beta=b/M$ with M being the total building (primary structure) mass. The expressions in (15) correspond to optimal tuning parameters for the classical TMD derived in closed-form in [22] that minimise the displacement response variance of white noise excited undamped single DOF primary structures in which the TMD mass ratio μ has been replaced by the sum of the mass ratio plus inertance ratio $\mu+\beta$. In this regard, these expressions do not yield, by any means, optimum TMDI design parameters for the herein adopted primary structure corresponding to any particular optimisation criterion. However, they do yield reasonable values for the stiffness and the damping properties of the TMDI which suffice for the purposes of the present parametric study.

In Fig. 4 the peak top floor displacement and acceleration of the TMDI equipped primary structure is plotted as a function of the inertance ratio $\beta=b/M$ for six values of the attached mass. The reported values are normalised by the corresponding peak value of the uncontrolled (no TMDI) structure. It is seen that the inclusion of the inerter becomes beneficial in terms of reducing the peak top floor displacement for the relatively small attached mass. In fact, for $\mu\geq$0.5% the classical TMD outperforms the TMDI for the whole range of β values considered. However, for the smaller attached mass, the inclusion of the inerter reduces the top floor displacements appreciably and it is seen that the smaller the attached mass, the more effective the inclusion of the inerter becomes. These trends confirm similar results reported in the literature for the case of earthquake excited building structures [11]. More importantly, interpreting the results in Fig. 4(a) from a performance-

based design viewpoint, it can be seen that the TMDI can achieve the same performance with larger mass classical TMD which suggests that the inclusion of the inerter leads to mass reduction or replacement for the same performance. For example, a TMDI with μ=0.1% and β=50% achieves the same performance in terms of peak floor displacement as the classical TMD with double the mass μ=0.2%.

Turning the attention to peak floor accelerations (Fig 4(b)), it is seen that for all the values of the attached mass considered, better vibration suppression performance is achieved with higher inertance values. For higher attached mass, this improvement is monotonic, but tends to saturate faster and is less significant compared to smaller attached mass. Overall, the results in Fig. 4 suggests that the TMDI is more effective in reducing floor accelerations than displacements and that it is wiser to combine large inertance values with small attached mass. This consideration allows for significant weight reduction in the overall passive control system and therefore gains in terms of axial gravity load accommodation for the primary structure. Moreover, given that floor accelerations are more critical than floor displacements for design verification at a serviceability limit state, it is practically more reasonable to pursue optimum design in terms of floor accelerations in practice, though, this aspect is not treated in this paper.

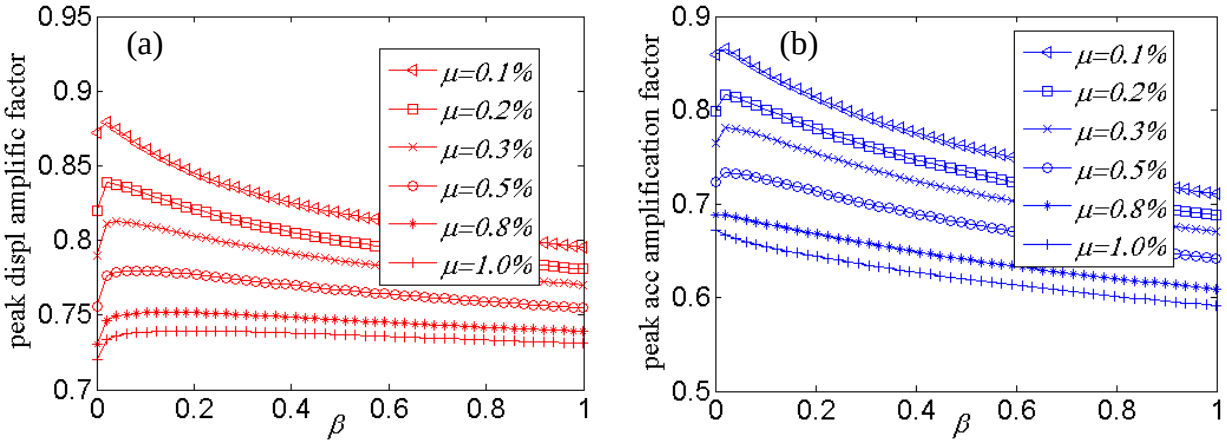

Figure 4- Peak top floor displacement (a) and acceleration (b) of TMDI equipped primary structure for different values of inertance ratio β=b/M and attached mass ratio μ= m_{TMDI}/M and normalised by the corresponding peak values of the uncontrolled structure.

Additional data of practical importance in structural design are furnished in Fig. 5. Specifically, Fig. 5(a) plots the peak attached mass displacement as a function of the inertance normalised by the value attained for b=0 (classical TMD). This response quantity is critical in the TMDI design as it relates to the damper and the inerter stroke (relative displacement of the device terminals), as well as with the required clearance between the attached mass and the host structure. It is seen that the inclusion of the inerter in the TMDI configuration yields significant reductions to the peak attached mass displacement (note the logarithmic scale in the y-axis of Fig. 5(a)), though the rate of this reduction reduces as the inertance value increases for the same attached mass (saturation). Lastly, Fig. 5(b) plots the peak force developed in the inerter as a function of the inertance. Following (1), this force is given as the product of the inertance value b with the peak relative acceleration in (13) between the DOF corresponding to the attached mass and the DOF of the penultimate floor. It is seen that this force attains a local maximum for β values dependent on the attached mass (β=20% on average for the attached mass herein considered) and then slightly reduces with increasing inertance. This is quite welcoming as the inerter force needs to be transferred to the primary structure and, therefore, high inerter forces would contribute to an increase of the TMDI installation cost compared to the classical TMD. In any case, aalthough local

detail design of the inerter-to-the-primary-structure connection falls well beyond the scope of this paper, it is important to note that the peak developing internal force of the inerter that needs to be transmitted locally to the primary structure is reasonable for the scale of the primary structure considered and no special provisions for local connection detailing would be required.

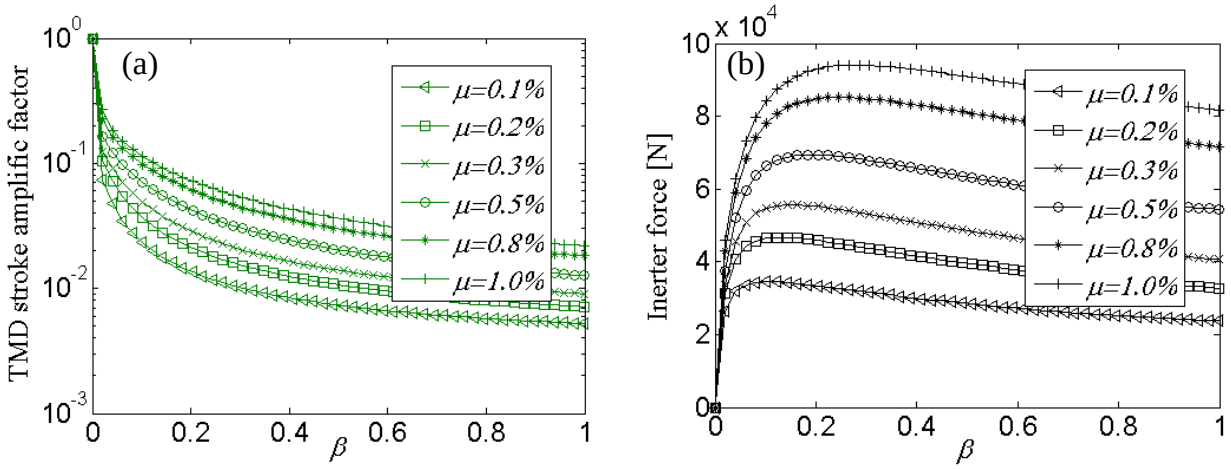

Figure 5- (a) Peak TMDI attached mass displacement normalised to the corresponding value for the classical TMD (β=0), and (b) Peak inerter force developed for different values of inertance ratio β=b/M and attached mass ratio μ= m_{TMDI}/M.

5 CONCLUDING REMARKS

The effectiveness of the tuned mass-damper-inerter (TMDI) vis-à-vis the classical tuned mass-damper (TMD) has been assessed to suppress wind induced vibrations in typical tall buildings in the across-wind direction. This was accomplished by undertaken a comprehensive parametric study involving a linear dynamical system defined defined by a diagonal mass matrix and full damping and stiffness matrices, which captures faithfully the dynamic properties of a detailed finite element model corresponding to a benchmark 74-storey building with square floor plan. This structural system is equipped with TMDIs of several different values of attached mass and inertance coefficients by elementary operations to the mass, damping, and stiffness matrices. The wind action is represented by an analytical spectral density matrix modelling correlated across-wind induced forces accounting for vortex shedding and the structural analysis step is undertaken in the frequency for efficiency. Using sub-optimal values for the frequency and damping TMDI ratios, it was found that the TMDI achieves better performance in terms of peak top floor acceleration reduction with increasing inertance than a classical TMD with the same attached mass. This is also true for relatively small attached masses of practical interest to tall buildings (less than 0.5% the total buildings mass) for the case of peak top floor displacements, though for larger attached masses the inclusion of the inerter is detrimental to floor displacement suppression. Further, it is shown that the TMDI reduces significantly the peak attached mass displacement, while the peak developing forces at the inerter are not excessive and can be locally accommodated by the building. Overall, the herein reported results demonstrate that the inclusion of the inerter to the classical TMD is more beneficial for small attached masses, while the same level of vibration suppression can be achieved with TMDIs of significantly smaller attached mass (and large inertance value) from the attached mass that the classical TMD would require. The latter leads to significant weight reductions to the overall passive vibration control system.

ACKNOWLEDGEMENTS

This work has been funded by EPSRC in UK, under grant EP/M017621/1. The authors gratefully acknowledge this financial support.

REFERENCES

[1] Liang, S., Liu, S., Li, Q.S., Zhang, L. & Gu, M. Mathematical model of across-wind dynamic loads on rectangular tall buildings, *Journal of Wind Engineering and Industrial Aerodynamics*, 2002; **90**:201-251.

[2] Ciampoli, M. & Petrini, F. (2012). Performance-Based Aeolian Risk assessment and reduction for tall buildings, *Probabilistic Engineering Mechanics*, 2012; **28**:75–84.

[3] Bernardini, E., Spence, S.M.J., Kwon, D.K. & Kareem, A. Performance-Based Design of High-Rise Buildings for Occupant Comfort. *Journal of Structural Engineering* 2015; **141**(10), Article number 04014244.

[4] Kwok, K.C.S, Hitchcock, P.A. & Burton, M.D. (2009). Perception of vibration and occupant comfort in wind-excited tall buildings. *Journal of Wind Engineering and Industrial Aerodynamics*, 2009; **97**: 368–380.

[5] Kareem, A., Kijewski, T. & Tamura, Y. Mitigation of motions of tall buildings with specific examples of recent applications. *Wind and Structures*, 1999; **2**(3): 201-251.

[6] Tse, K.T., Kwok, K.C.S. & Tamura, Y. Performance and Cost Evaluation of a Smart Tuned Mass Damper for Suppressing Wind-Induced Lateral-Torsional Motion of Tall Structures. *Journal of Structural Engineering*, 2012; **138**(4): 514-525.

[7] Rana, R. & Soong, T.T. Parametric study and simplified design of tuned mass dampers. *Engineering Structures*, 1998; **20**(3): 193-204.

[8] Li, Q., Cao, H., Li, G., Li, S. & Liu, D.. Optimal design of wind-induced vibration control of tall buildings and high-rise structures. *Wind and Structures*, 1999; **2**(1): 69-83.

[9] De Angelis, M., Perno, S. & Reggio, A. Dynamic response and optimal design of structures with large mass ratio TMD. *Earthquake Engineering and Structural Dynamic*, 2012; **41**: 41–60.

[10] Marian, L. & Giaralis, A. Optimal design of inerter devices combined with TMDs for vibration control of buildings exposed to stochastic seismic excitations. *Proceedings of the 11th ICOSSAR International Conference on Structural Safety and Reliability for Integrating Structural Analysis, Risk and Reliability*, 1025-1032, *CRC Press*, 2013.

[11] Marian, L. & Giaralis, A. Optimal design of a novel tuned mass-damper–inerter (TMDI) passive vibration control configuration for stochastically support-excited structural systems. *Probabilistic Engineering Mechanics*, 2014; **38**: 156–164.

[12] Smith, M.C. Synthesis of Mechanical Networks: The Inerter. *IEEE Transactions On Automatic Control*, 2002; **47**(10): 1648-1662.

[13] Evangelou, S., Limebeer, D.J.N., Sharp, R.S. & Smith, M.C. Steering compensation for high-performance motorcycles. *IEEE Conf. Decision Control* 2004; **43**: 749-754.

[14] Wang, F.C., Hong, M.F. & Lin, T.C. Designing and testing a hydraulic inerter. *Proc. Inst. Mech. Eng. Part C J. Mech. Eng. Sci.* 2010; **1**(1): 1–7.

[15] Swift, S. J., Smith, M. C., Glover, A. R., Papageorgiou, C., Gartner, B. & Houghton, N. E. Design and modelling of a fluid inerter. *International Journal of Control*, 2013; **86**(11): 2035–2051.

[16] Giaralis, A. & Taflanidis A.A. Reliability-based design of tuned-mass-damper-inerter (TMDI) equipped stochastically support excited structures. *Proceedings of the 12th International Conference on Applications of Statistics and Probability in Civil Engineering- ICASP12*, 2015. Available at https://open.library.ubc.ca/cIRcle/collections/53032/items/1.0076257 (accessed 22 April 2015).

[17] Spence, S.M.J. & Gioffrè, M. Large scale reliability-based design optimization of wind excited tall buildings. Probabilistic Engineering Mechanics, 2012; 28: 206-215.

[18] Petrini, F. & Ciampoli, M. Performance-based wind design of tall buildings. *Structure & Infrastructure Engineering - Maintenance, Management, Life-Cycle Design & Performance*, 2012; 8(10), 954-966.

[19] Chopra, A.K. Dynamics of Structures: *Theory and Applications to Earthquake Engineering*. Prentice-Hall International Series in Civil Engineering and Engineering Mechanics 2000.

[20] Roberts J.B. & Spanos P.D. *Random Vibration and Statistical Linearization*. Dover, 2003.

[21] Davenport, A.G. Note on the distribution of the largest value of a random function with application to gust loading. *Proceedings of the Institution of Civil Engineers*, 1964; **28**(2), 187-196.

[22] Warburton, G.B. Optimal absorber parameters for various combinations of response and excitation parameter. *Earthquake Engineering and Structural Dynamics*, 1982; **10**: 381–400.

[23] Giaralis, A. & Marian, L. Use of inerter devices for weight reduction of tuned mass-dampers for seismic protection of multi-story building: the Tuned Mass-Damper-Interter (TMDI). *Proceedings SPIE 9799, Active and Passive Smart Structures and Integrated Systems 2016*, 97991G; doi:10.1117/12.2219324.